Inhibition and enhancement of cesium two-photon transition under control field

Yi-Chi Lee,[1,2,3] Ying-Yu Chen,[2] Chun-Ju Wang,[2] Hsiang-Chen Chui,[1,4] Li-Bang Wang,[5] and Chin-Chun Tsai,[1,2,*]

[1]*Department of Photonics, National Cheng Kung University, Tainan 70101, Taiwan*
[2]*Department of Physics, National Cheng Kung University, Tainan 70101, Taiwan*
[3]*Beam Dynamics Group, National Synchrotron Radiation Research Center, Hsinchu 30077, Taiwan*
[4]*Advanced Optoelectronic Technology Center, National Cheng Kung University, Tainan 70101, Taiwan*
[5]*Department of Physics, National Tsing Hua University, Hsinchu 30013, Taiwan*
[*] *chintsai@mail.ncku.edu.tw*

Abstract: The probability of two-photon transition (TPT) under a control field to inhibit the quantum interference and enhance the nonlinear optical cross section is observed. Essentially, this is a V-type electromagnetically induced transparency (EIT) with TPT instead of one photon transition. Numerical simulation based on solving the steady state density matrix can qualitatively fit the experimental data. A model of double-Lorentzian profile is used to fit the observed spectrum and give the de-convolution information of the inhibition of TPT spectrum due to EIT and enhancement on the wings of TPT. The frequency shift of the inhibit center is linear to the intensity of the control field (one-photon) and quadratic to the intensity of probe field (two-photon). Under the control field, a factor of 10 enhancements on the wings of the TPT is observed.

OCIS codes: (020.3690) Line shapes and shifts; (270.4180) Multiphoton processes; (300.6210) Spectroscopy, atomic.

References and links

1. S. E. Harris, J. E. Field, and A. Imamoglu, "Nonlinear optical processes using electromagnetically induced transparency," Phys. Rev. Lett. **64**(10), 1107–1110 (1990).
2. K. J. Boller, A. Imamolu, and S. E. Harris, "Observation of electromagnetically induced transparency," Phys. Rev. Lett. **66**(20), 2593–2596 (1991).
3. J. E. Field, K. H. Hahn, and S. E. Harris, "Observation of electromagnetically induced transparency in collisionally broadened lead vapor," Phys. Rev. Lett. **67**(22), 3062–3065 (1991).
4. A. Aspect, E. Arimondo, R. Kaiser, N. Vansteenkiste, and C. Cohen-Tannoudji, "Laser cooling below the one-photon recoil by velocity-selective coherent population trapping," Phys. Rev. Lett. **61**(7), 826–829 (1988).
5. S. E. Harris and Y. Yamamoto, "Photon switching by quantum interference," Phys. Rev. Lett. **81**(17), 3611–3614 (1998).
6. M. O. Scully, S. Y. Zhu, and A. Gavrielides, "Degenerate quantum-beat Laser-lasing without inversion and inversion without lasing," Phys. Rev. Lett. **62**(24), 2813–2816 (1989).
7. S. E. Harris, "Lasers without inversion-interference of lifetime-broadened resonances," Phys. Rev. Lett. **62**(9), 1033–1036 (1989).
8. G. S. Agarwal, G. Vemuri, and T. W. Mossberg, "Lasing without Inversion-Gain Enhancement through Spectrally Colored Population Pumping," Phys. Rev. A **48**(6), R4055–R4058 (1993).
9. G. G. Padmabandu, G. R. Welch, I. N. Shubin, E. S. Fry, D. E. Nikonov, M. D. Lukin, and M. O. Scully, "Laser oscillation without population inversion in a sodium atomic beam," Phys. Rev. Lett. **76**(12), 2053–2056 (1996).
10. G. S. Agarwal and W. Harshawardhan, "Inhibition and enhancement of two photon absorption," Phys. Rev. Lett. **77**(6), 1039–1042 (1996).
11. S. F. Yelin, V. A. Sautenkov, M. M. Kash, G. R. Welch, and M. D. Lukin, "Nonlinear optics via double dark resonances," Phys. Rev. A **68**(6), 063801 (2003).
12. H. Wang, D. Goorskey, and M. Xiao, "Enhanced Kerr nonlinearity via atomic coherence in a three-level atomic system," Phys. Rev. Lett. **87**(7), 073601 (2001).
13. C. J. Foot, *Atomic Physics,* Oxford master series in physics (Oxford University Press, 2005).
14. Y. C. Lee, H. C. Chui, Y. Y. Chen, Y. H. Chang, and C. C. Tsai, "Effects of light on cesium 6S-8S two-photon transition," Opt. Commun. **283**(9), 1788–1791 (2010).

#166934 - $15.00 USD Received 18 Apr 2012; revised 11 May 2012; accepted 5 Jun 2012; published 13 Jun 2012

15. J. Y. Gao, S. H. Yang, D. Wang, X. Z. Guo, K. X. Chen, Y. Jiang, and B. Zhao, "Electromagnetically induced inhibition of two-photon absorption in sodium vapor," Phys. Rev. A **61**(2), 023401 (2000).
16. M. Yan, E. G. Rickey, and Y. F. Zhu, "Observations of absorptive photon switching and suppression of two-photon absorption in cold atoms," J. Mod. Opt. **49**(3-4), 675–685 (2002).
17. R. Y. Chang, Y. C. Lee, W. C. Fang, M. T. Lee, Z. S. He, B. C. Ke, and C. C. Tsai, "A narrow window of Rabi frequency for competition between electromagnetically induced transparency and Raman absorption," J. Opt. Soc. Am. B **27**(1), 85–91 (2010).

1. Introduction

The phenomenon of electromagnetically induced transparency (EIT) was first proposed by Harris, Field, and Imamoğlu in 1990 [1]. A medium exhibiting EIT possesses a steep dispersion and becomes transparent for a resonant laser field over a narrow spectral range. Spectroscopic investigation of the interaction between the three-level system and two resonant monochromatic radiations reveals a rich source of interesting physics. The quantum interference of the transition pathways leads to the formation of EIT [2, 3]. Under this EIT configuration, the ability to modify the absorption and susceptibility of the transition via the real or imaginary part of the solution of the density matrix has attracted considerable attention. The drastic enhancement of the dispersion near resonance has tamed the photon successfully, i.e. the storage of light inside the medium, providing a stable platform for the generation and transportation of quantum information [4, 5]. The new transition path-way could be viewed as a "tuning knob" which is mediated by the atomic coherence in order to interfere with the occurrence of the original transition scheme. The ability to greatly modify the transition susceptibility has attracted considerable attention in a variety of physical fields, including the cooling of atoms below the photon recoil limit [6], lasing without population inversion [7–9]. Furthermore, coherence effects such as two-photon inhibition and enhancement [10] (discussed in the next sections), evolution of double dark states [11], photon switching [5], and Kerr nonlinearity [12] have been exhibited.

We report a quantum interference phenomenon observed in the one-color two-photon transition (TPT) of ^{133}Cs atom. In the TPT scheme, the inhibition and enhancement effects have been observed due to the presence of a control field. The modification of the two-photon absorption by a coherent control field may have some application, such as two-photon lasing or enhancing the nonlinear coefficient χ^2 in the gain media. Considering the interaction process, a V-type three-level atomic system which was acted upon by two laser fields is shown in Fig. 1. Resonant direct two-photon absorption passes through a virtual state is induced by a probe beam driven from |6S, F = 4> →|8S, F = 4> transition. The other laser beam denoted as control laser is driving the population from |6S, F = 4> →|6P, F = 4>. Without the existence of control laser, the mechanism in the system is typically a TPT of ^{133}Cs $6S_{1/2}$ to $8S_{1/2}$.

The inhibition and enhancement of TPT are based on the concept presented in [10]. Gao and associates have performed similar experiment on sodium atoms [13] while the result on rubidium atoms has been reported by Yan et al. [14]. However, they used two-color resonant lasers as the probe path way. To our knowledge, this is the first demonstration of the inhibition and enhancement of one-color TPT.

#166934 - $15.00 USD Received 18 Apr 2012; revised 11 May 2012; accepted 5 Jun 2012; published 13 Jun 2012

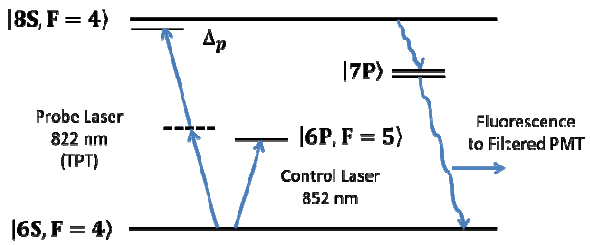

Fig. 1. Energy diagram of the TPT V-type EIT in cesium atomic system. The corresponding laser wavelengths of probe and control fields are labeled. Cascade fluorescence is collected to monitor the population of the 8S level.

2. Experiments

The experimental block diagram is shown in Fig. 2. In this experiment, the probe laser is from a single-mode ring-cavity Ti-sapphire laser (Coherent 899-29) pumped by a 10-watt diode pumped solid state laser (Coherent Verdi-10). The Ti-sapphire laser is frequency-stabilized to a thermo-stabilized reference cavity and the resulting linewidth is approximately 500 kHz (root mean square). The laser beam size inside the Cs cell is 1 mm in diameter. The wavelength of the probe laser is tuned to 822 nm to induce the TPT of the cesium atoms from $6S_{1/2}$ to $8S_{1/2}$ states. The control laser is from an external cavity diode laser at 852 nm with a total power of 50 mW. Frequency of this control laser is locked on the cesium D2 line ($|6S_{1/2}$, $F = 4\rangle \rightarrow |6P_{3/2}$, $F = 5\rangle$) by saturation absorption in a vapor cell. The linewidth of the control laser is approximately 1 MHz. To overlap the control and probe laser beams, a half wave plate and a polarization beam splitter cube are used in the experiment as shown in Fig. 2. Without the interaction of the control laser, we obtain the typical spectrum of cesium 6S-8S TPT and the measured linewidth is approximately 2 MHz at a laser power of 10 mW and is 3 MHz when the laser power is increased to 100 mW.

In the experimental setup, the probe laser beam is amplitude-modulated by a mechanical chopper at 1.15 kHz. In order to accurately locate the frequency of the absorption dip caused by the control laser, a beam splitter is used to split the probe beam into two parts. One of the beams is directed into a cesium vapor cell (called the reference cell) in which the normal TPT signal is recorded. This serves as a frequency reference where the frequency of the TPT can be precisely determined. The other beam is directed into another identical vapor cell (called the main cell). The laser beams are reflected back by a plane mirror and are then overlapped with the incoming beam within the cell. Two plano-convex lenses (f = 150 mm) are put outside each cell in a confocal arrangement to increase the laser intensity in the interaction region. The 852 nm control laser is also directed into the main cell and is overlapped with one of the probe beam. Both cells are temperature-stabilized within ± 0.1 þC. The temperature of the cell body is raised to 65 þC and the temperature of the cold finger is about 10 degree lower than the cell body. The vapor pressure in the cell is maintained at approximately 10^{-5} Torr. Great care has been taken to ensure all the parameters of the reference cell is the same as those of the main cell so that unwanted systematic effects, such as pressure shift and broadening, and light shift can be avoided. The diameter of the laser beam in the center of the interaction region is measured to be 68 μm. Once the TPT occurs, cascade fluorescence from 7P-6S at 455.5 nm and 459.3 nm is collected by an imaging system including two lens (f = 25 mm), two interference filters (Andover 456FS10-25) and a slit for filtering the background light. The fluorescence light due to cascade decay from the upper-excited state $8S_{1/2}$ is proportional to the absorption rate of the two-photon absorption and is thus a signature of the

#166934 - $15.00 USD Received 18 Apr 2012; revised 11 May 2012; accepted 5 Jun 2012; published 13 Jun 2012

TPT. The emitted photons are detected by a photomultiplier tube (Hamamatsu R928) and the photon signals from both cells are sent to two lock-in amplifiers (Stanford Research System 830) for demodulation. The two output signals from the lock-in amplifiers are recorded simultaneously by a digital oscilloscope (Tektronix TDS220) and are processed by a computer.

The suppression of TPT is observed in the main cell. The condition of the control laser, such as the intensity and detuning are varied and its effect on the suppression of the two-photon absorption is investigated. This suppression phenomenon can be regarded as a destructive interference between different channels in the two photon transition. There are intermediate dressed states induced by the control field and the interfering quantum paths among the bare atomic states can suppress both the single-photon absorption and the two-photon absorption [15, 16]. The data analysis and theoretical explanation of the phenomenon are described in the following sections.

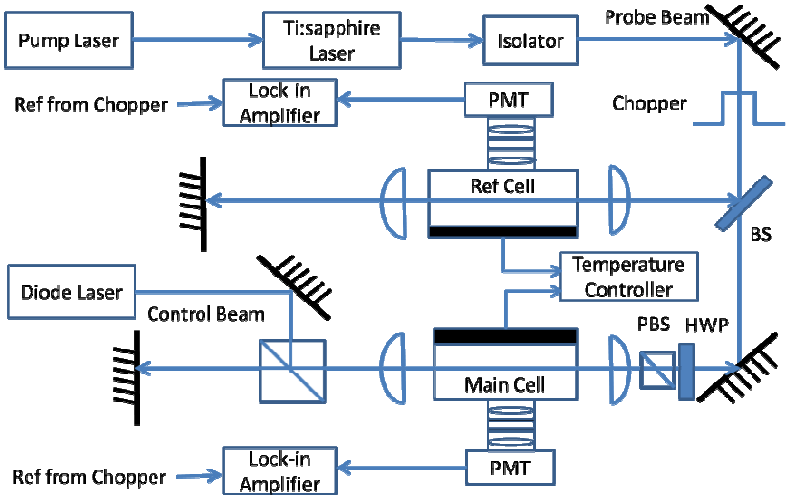

Fig. 2. The schematic diagram of the experimental setup for the suppression of the two-photon V-type EIT transition. HWP: Half-wave plate, PBS: polarizing beam splitter, BS: beam splitter and PMT: photomultiplier tube.

3. Theoretical simulations

The density matrix of this V-type three-level TPT system is presented as follows:

$$i\hbar\dot{\rho} = [\mathrm{H}, \rho] - \tfrac{i\hbar}{2}\{\Gamma, \rho\} \qquad (1)$$

where ρ is the density matrix that contains all of the information about the system (including the population of the atomic system and the optical property of the photon fields), H is the interaction Hamiltonian and Γ characterizes the decay process. The more detailed descriptions were showed in Ref [17]. As shown in Fig. 1, these three levels are $|6S_{1/2}, F = 4\rangle \rightarrow |8S_{1/2}, F\rangle$ (level 1 to level 2) coupled by TPT, and $|6S_{1/2}, F = 4\rangle \rightarrow |6P_{3/2}, F = 5\rangle$ (level 1 to level 3) coupled by the control field. Therefore, the Hamiltonian can be written as,

$$\mathrm{H} = \begin{pmatrix} 0 & -\frac{\Omega_p}{2}e^{i\Delta_p t} & -\frac{\Omega_c}{2}e^{i\Delta_c t} \\ -\frac{\Omega_p}{2}e^{-i\Delta_p t} & 0 & 0 \\ -\frac{\Omega_c}{2}e^{-i\Delta_c t} & 0 & 0 \end{pmatrix}$$

, where Ω_p, Ω_c are the Rabi frequency of the probe and control fields, Γ_2, Γ_3 are the decay rate of $8S_{1/2}$ and $6P_{3/2}$ states, and Δ_p, and Δ_c are the detuning of the probe and control laser frequency to atomic resonance transitions. In the

#166934 - $15.00 USD Received 18 Apr 2012; revised 11 May 2012; accepted 5 Jun 2012; published 13 Jun 2012

decay processes, fields linewidth γ_p and γ_c are included as a de-coherence source. Under weak probe strength, the probe beam absorption can be presented explicitly by the imaginary part of ρ_{12}.

$$\mathrm{Im}[\rho_{12}]=\frac{-\Omega_p\Gamma_2\Gamma_3^2-\Omega_p\Omega_c^2\Gamma_3-4\Omega_p\Gamma_2(\Delta_p+\Delta_c)^2}{\Gamma_2^2\Gamma_3^2+\Omega_c^4+16\Delta_p^2(\Delta_p+\Delta_c)^2+2\Gamma_2\Gamma_3\Omega_c^2-8\Omega_c^2\Delta_p(\Delta_p+\Delta_c)+4\Gamma_3^2\Delta_p^2+4\Gamma_2^2(\Delta_p+\Delta_c)^2} \quad (2)$$

In this experiment, the control field is on resonance, i.e., $\Delta_c = 0$.

The steady-state solution of Eq. (1) also can be obtained numerically. The imaginary part of ρ_{12} represents the absorption of level 1 to level 2 corresponding to the probe beam absorption (TPT). Under varies Rabi frequencies of probe and control fields, this absorption Im[ρ_{12}] changes from EIT to Raman absorption within a quite narrow Rabi frequency regime [17]. To obtain an EIT spectrum, a weak probe and strong control fields are required (Ω_p to Ω_c about 10 to 1).

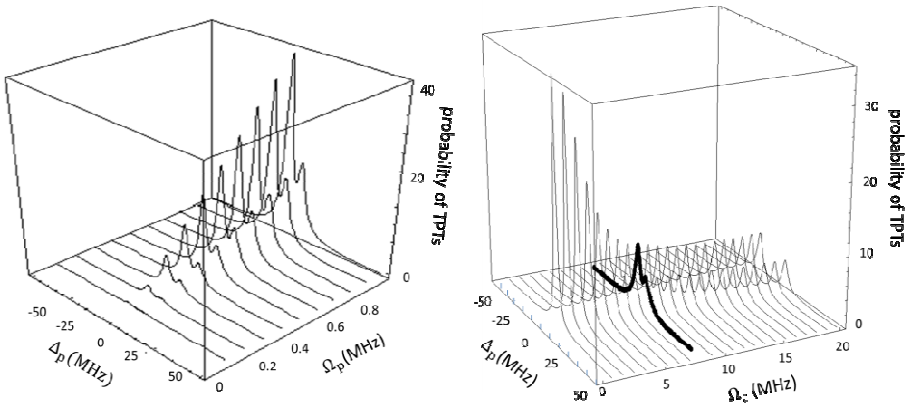

Fig. 3. The simulation spectra of the probability of TPTs under the presence of control field. (a) The probability of TPTs as a function of the probe detuning under various Rabi frequencies of probe field. The Rabi frequency of the control field is fixed at 7.35 MHz. (b) The probability of TPTs as a function of the probe detuning under various Rabi frequencies of control field. The Rabi frequency of the probe field is fixed at 0.1 MHz. The heavy solid line is the recorded spectrum where the Rabi frequency Ω_p and Ω_c are the corresponding experimental conditions and peak height is normalized to the simulation.

Figure 3 shows the simulation spectra of the probability of TPT under the presence of the control field. The parameters used in the simulation are adapted from literature of the experimental setting. In Fig. 3(a), the probability of TPT as a function of probe detuning under various Rabi frequencies of the probe is plotted and the Rabi frequency of the control field is fixed at 7.35 MHz. Figure 3(b) on the other hand, shows the probability of TPT as a function of the probe detuning under various control Rabi frequencies, while this time the Rabi frequency of the probe field is fixed at 0.1 MHz. From the simulation results, the shape of the inhibition spectra is almost unchanged when the probe Rabi frequency (Ω_p) is increasing as shown in Fig. 3(a). However, the shape of the inhibition spectrum is clearly sensitive to the Rabi frequency (Ω_c) of the control field as shown in Fig. 3(b). By increasing the Rabi frequency of the control field, the spectrum shows from an enhancing broadening to an inhibition dip and then doublet peaks. The doublet peaks are called the Aulter-Townes splitting which occurs in strong control field regime where the coherence of EIT interference is destroyed. However, although laser intensity of TPT is high, the Rabi frequency Ω_p is still weak due to the very low cross section of TPT. Therefore, no Aulter-Townes splitting is

#166934 - $15.00 USD Received 18 Apr 2012; revised 11 May 2012; accepted 5 Jun 2012; published 13 Jun 2012

generated in the laser intensity used in this experiment. The heavy solid line in Fig. 3(b) is the recorded spectrum where the Rabi frequency Ω_p and Ω_c are the corresponding experimental conditions and peak height is normalized to the simulation. Other related simulation conditions are shown as below: Γ_2 = 5.22 MHz (decay rate of the $6P_{3/2}$), Γ_3 = 2.18 MHz (decay rate of the $8S_{1/2}$), γ_p = 1 MHz (the linewidth of the probe beam), and γ_c = 1 MHz (the linewidth of the control beam).

Solving the steady state solution of density matrix function to fit the curve, one can determine the line profile and analyze the subtraction of the inhibited two-photon fluorescence signals. A model of double-Lorentzian function is used to fit the two-photon fluorescence (positive) and the inhibition dip (negative) for analyzing the recorded spectrum. Factoring the imaginary part of ρ_{12} in Eq. (2), one can show that the solution of steady state density matrix is equivalent the double Lorentzian model [shown in Appendix]. Fitting the spectrum with a double Lorentzian gives the information of peak position and linewidth for both two-photon fluorescence and the inhibition dip directly. The equation is shown as followed:

$$y = \left\{ y_a + \frac{2A_1}{\pi} \frac{\gamma_1}{4(x-\omega_1)^2 + \gamma_1^2} \right\} - \left\{ y_b + \frac{2A_2}{\pi} \frac{\gamma_2}{4(x-\omega_2)^2 + \gamma_2^2} \right\} \qquad (3)$$

where y_a, y_b are the backgrounds, A_1, A_2 are the amplitudes, ω_1, ω_2 are the center frequencies, and γ_1, γ_2 are the full width at half maximum (FWHM) of these two Lorentzian curves.

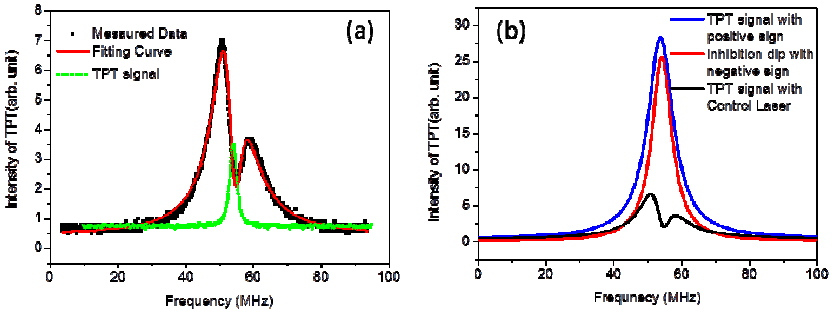

Fig. 4. Measured two-photon fluorescence intensity versus the probe detuning Δ_p with the presence of control field. (a) The suppression of TPT spectrum due to destructive interference is shown in black dots and the fitting results according to Eq. (3) in red. The Rabi frequency of the control laser (Ω_c) is about 7.65 MHz. On the bottom showing in green is the typical TPT signal without the control field obtained from reference cell. (b) The subtraction using a double-Lorentzian model (black line) and their original Lorentzian profiles, TPT signal (blue line) with positive sign and inhibition dip (red line) with negative sign.

The subtraction spectra are shown in Fig. 4. Figure 4(a) shows the recorded spectrum of TPT as a function of the probe detuning Δ_p (black dots). The frequency of control field is locked to the hyperfine transition of $|6S_{1/2}, F = 4\rangle \rightarrow |6P_{3/2}, F = 5\rangle$ However, there is about 1 MHz off resonance due to the offset of error signal which makes the inhibition dip on the blue side. The red solid line is the subtraction of Eq. (3). A pure TPT signal recorded simultaneously from the reference cell is plotted in green for comparison. Figure 4(b) shows the subtraction using a double-Lorentzian model (black line) and their original profiles, TPT signal (blue line) with positive sign and inhibition dip (red line) with negative sign. The fitting result is plotted in Fig. 4(a) (red line) and gives the fitting parameters ω_1 and ω_2 to be 53.77 MHz and 54.18 MHz. γ_1 and γ_2 are 9.18 MHz and 7.10 MHz respectively. The residue of fitting shows a good agreement and indicates no systematic error.

#166934 - $15.00 USD Received 18 Apr 2012; revised 11 May 2012; accepted 5 Jun 2012; published 13 Jun 2012

4. Data analysis

In order to record the signal of TPT, the frequency of the Ti:sa laser named probe beam (ω_p) was scanned to make $\omega_p + \omega_p$ across the cesium $|6S_{1/2}, F = 4\rangle \rightarrow |8S_{1/2}, F = 4\rangle$ transition. A counter-propagating control laser was superimposed with the TPT beam. Figure 4(a) shows the measured two-photon cascade fluorescence (green line) from the reference cell and the TPT under the control field (black dots) from the main cell versus the probe frequency detuning. The signal of pure TPT from the reference cell is used for comparing the linewidth and transition intensity with the TPT under the interaction of the control field. The linewidth of the TPT was reported approximately 1.5 to 2.0 MHz [13, 14]. However, under the interaction of control field, the linewidth is greatly broadened. By the fitting parameters of the spectrum as shown in Fig. 4(b), one can obtain the center frequencies (ω_1, ω_2) and the corresponding linewidth (γ_1, γ_2) of the two curves. The difference of these two peaks ($\Delta f = \omega_1 - \omega_2$) and the corresponding linewidth (γ_1, γ_2) are changed while varying the intensity of probe field or control field. Next, we will discuss the intensity dependence of these suppression spectra.

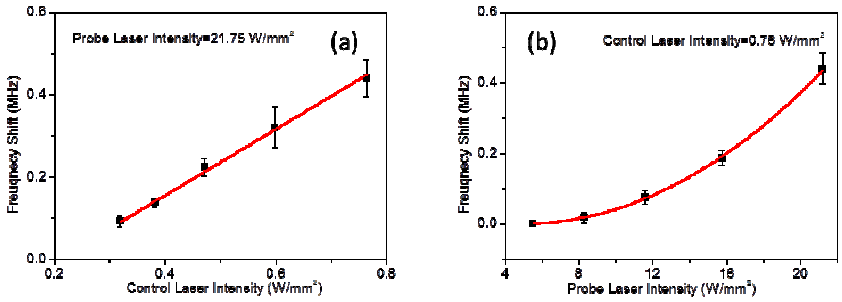

Fig. 5. (a) The frequency shift Δf versus the intensity of the control field with the probe intensity fixed. Solid line is a linear fit. (b) The frequency shift Δf versus the probe field intensity. Solid line is a quadratic fit.

The frequency shift Δf indicates the inhibition center respective to the TPT. The dependence of the inhibition center on the intensity of the control field is plotted in Fig. 5(a) while the intensity of the probe field is fixed at 79 mW/cm^2. The solid line is a linear fit. It is clear that the dependence is linear since the control filed is a one photon resonance. Actually, the frequency shift of these two curves (ω_1, ω_2) is increasing with different rates with the intensity of the control field, frequency shift of the y_a curve is −274.3 kHz/mW, and the shift of the y_b curve −174 kHz/mW. When the intensity of the control laser is stronger, the signal to noise ratio of recorded spectra is higher. However, the center positions are disturbed due to de-coherence by the control field. Therefore, the error bars of Δf are larger. Figure 5(b) shows the frequency shift Δf with changing the intensity of the probe field while keeping the intensity of the control field at 6 mW/cm^2. It is a quadratic dependence since the probe field is a TPT. As we can see in Fig. 5(a), a larger error bars arose from a higher probe field because the high probe intensity destroys the quantum interference.

Fitting the linewidth versus the intensity of control field and probe field is shown in Fig. 6. In Fig. 6(a), the linewidth of both curves (γ_1, γ_2) is increasing linearly with the intensity of the control filed. It reaches its saturation intensity at the last point. Figure 6(b) shows the linewidth of both curves (γ_1, γ_2) versus the intensity of probe field. It is clear that the linewidth of both curves (γ_1, γ_2) does not change much. Although the probe intensity is about a hundred times larger than that of the control field, they do not exhibit power broadening due to the weak of TPT probability.

#166934 - $15.00 USD Received 18 Apr 2012; revised 11 May 2012; accepted 5 Jun 2012; published 13 Jun 2012

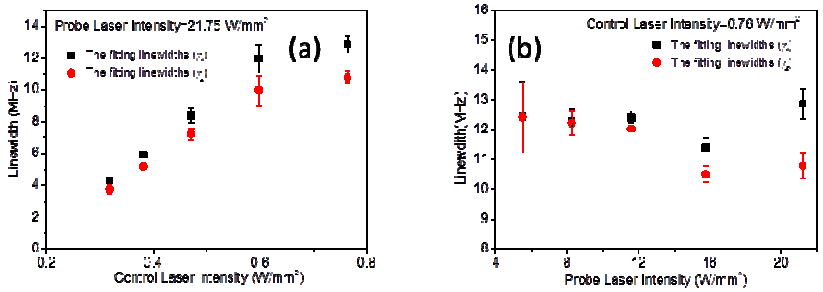

Fig. 6. (a) The fitting linewidth (γ_1, γ_2) versus the probe intensity, and (b) the fitting linewidth (γ_1, γ_2) versus TPT intensity. Red: γ_1, and Black: γ_2.

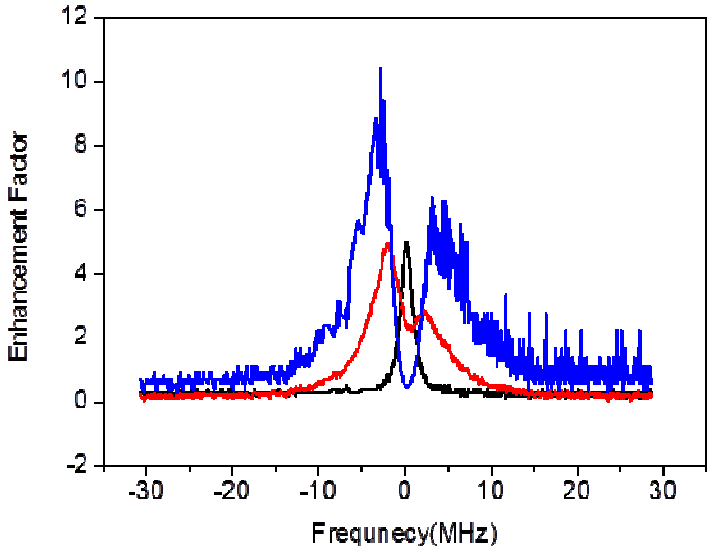

Fig. 7. Recorded spectrum with pure TPT (in black from reference cell) and the present of control field (in red from the main cell). The ratio of these two signals (in blue) shows the enhancement on the wings and the depletion on the center of the TPT affected by the control field.

The effect of the control field not only creates the destructive quantum interference at the center of TPT but also arise an enhancement of the TPT on the wings. In Fig. 7, the pure TPT (in black) and the TPT with the presence of control field (in red) are recorded simultaneously while scanning the frequency of TPT. The ratio of these two signals (in blue) (the peaks height is normalized to one) shows a clear depletion at the center and an almost 10 fold enhancement on both wings. This enhancement is due to the nonlinear effects with the present of control field. It has been discussed in ref [10]. When the Rabi frequency of the probe field increases and hence the optical nonlinearity, the coherence of the quantum interference will be destroyed, as shown in Fig. 3(b). For the probe Rabi frequency larger than 10 MHz, the splitting becomes wider and forms an Autler-Townes doublet since the interference between TPT and probe field being destroyed. However, this phenomenon will occur at much higher intensity of control filed due to its weak transition probability.

#166934 - $15.00 USD Received 18 Apr 2012; revised 11 May 2012; accepted 5 Jun 2012; published 13 Jun 2012

5. Conclusions

This study describes a pure TPT under a control field to create quantum interference and nonlinear enhancement phenomena. Unlike most papers describing the two-color TPT with control field, the one-color TPT with control configuration yields more control in regards to quantum interference by a destructive coherence effect and enhancing nonlinear optical properties. A numerical simulation based on solving the steady state solution of density matrix can qualitatively fit the experimental data. A model of double-Lorentzian profile (equivalent to the imaginary part of ρ_{12}) is used to fit the observed spectrum and give the information of the TPT (positive Lorentzian), inhibition effect (negative Lorentzian), and power dependence of linewidth and light shift. The control field is from a Cs D2 line transition which has relatively strong oscillator strength. From our previous study [17], controlling the Rabi frequency of Cs D2 line can either create EIT, or electromagnetically induced absorption (EIA), or destroy the coherence process. However, the TPT has relatively weak oscillator strength. Therefore, under the laser power generated from a Ti:sapphire laser (about 100 mW inside the cell), it is still in the weak probe regime. Increasing the intensity of control field, we see an enhancement on the wings of TPT and then the destruction of the quantum interference on the transition center.

Appendix:

(1) In Eq. (2) for $\Delta_c = 0$, we have

$$\mathrm{Im}[\rho_{12}]=\frac{-4\Omega_p\Gamma_2\Delta_p^2-\Omega_p\Gamma_2\Gamma_3^2-\Omega_p\Omega_c^2\Gamma_3}{16\Delta_p^4+4(\Gamma_3^2+4\Gamma_2^2-2\Omega_c^2)\Delta_p^2+\Gamma_2^2\Gamma_3^2+\Omega_c^4+2\Gamma_2\Gamma_3\Omega_c^2}$$

(2) To factoring the imaginary part of ρ_{12} into a double Lorentzian form, one can assume that denominator is the product of $((A\Delta_p^2+B)^2+C^2)((D\Delta_p^2+E)^2+F^2)$, where A, B, C, D, E, and F are constants to be determined.

(3) Compared the coefficients and set A = D = 2, and then, the results are $E=-B$, $B^2=\Omega_c^2-\frac{1}{4}(\Gamma_2-\Gamma_3)^2$ and $C^2=F^2=\frac{1}{4}(\Gamma_2+\Gamma_3)^2$.

(4) Then the double Lorentzian will be $\frac{G}{(A\Delta_p^2+B)^2+C^2}+\frac{H}{(D\Delta_p^2+E)^2+F^2}$.

Acknowledgments

We wish to acknowledge the support of this work by the National Science Council, Taiwan under contact no. NSC 98-2112-M-006-004-MY3. We also thank Mr. Jason Prahl for his English editorial assistance.

#166934 - $15.00 USD Received 18 Apr 2012; revised 11 May 2012; accepted 5 Jun 2012; published 13 Jun 2012